The Vitória Eddy and Its Relation to the Brazil Current

CLAUDIA SCHMID,* HARTMUT SCHÄFER,* GUILLERMO PODESTÁ,** AND WALTER ZENK*

*Institut für Meereskunde an der Universität Kiel, Kiel, Germany
**Rosenstiel School of Marine and Atmospheric Sciences, University of Miami, Miami, Florida

(Manuscript received 5 April 1994, in final form 5 December 1994)

ABSTRACT

In late austral summer 1991 a cyclonic thermocline eddy was detected in the subtropical western South Atlantic off the Brazilian shelf near the city of Vitória. This Vitória eddy was tracked for 55 days by surface drifters drogued at 100-m depth. The drifters had been deployed in the western boundary current regime by FS *Meteor* as part of a basinwide surface current study. The analysis of a combined CTD/XBT section across the Vitória eddy, together with drifter data and satellite images of the thermal surface structure revealed the unexpected complexity of the region. The eddy interacted not only with the local topography and the Brazil Current, located farther offshore, but also with an extended upwelling regime north of Cabo Frio. The hydrographic and kinematic properties and anomalies of the Vitória eddy are analyzed and compared with similar vortices described elsewhere in literature.

1. Introduction

The Brazil Current represents the western boundary of the subtropical circulation in the South Atlantic. Between 20° and 30°S, its transport appears to be considerably smaller than that of analogous current systems in the Southern Hemisphere, for example, the Agulhas and East Australian Currents. A large uncertainty exists about the spatial and temporal variability of the Brazil Current (Peterson and Stramma 1991). The Brazil Current appears to be a continuous feature associated with the continental margin (north of the confluence zone), a region where traditionally shelf oceanography ends and "blue water" oceanography begins. This might be a reason for a long-lasting deficit in Brazil Current observations. The situation has changed considerably with the advent of satellite oceanography. In a recent study, Garfield (1990) analyzed large quantities of infrared images of the Brazil Current. In comparison with hydrographic data he showed that, between 20° and 31°S, the continuous Brazil Current is associated with eddies and meanders and forms fronts west of the main stream. He concluded that "within the error of measurements the satellite-derived boundary is a good representation of the near surface inshore Brazil Current front," and that "the shelf break accurately locates the mean position of this front." Since the thermal front appeared to be situated inshore of the 200-m isobath about half of the time, he was convinced that significant portions of the warm surface flow over the shelf had not been considered in historical calculations of the Brazil Current transport.

During the METEOR 15 Cruise in February 1991, a section was taken across the Brazil Current at 20.5°S near the port of Vitória, Brazil, south of the Vitória–Trindade Ridge (Fig. 1). This research was part of the Deep Basin Experiment, a subprogram of WOCE (Siedler and Zenk 1992). The thermal data collected during the cruise (Fig. 2a) revealed a cold core eddy closely tied to the subsurface bight formed by the meridional shelf edge and the northern chains of the Vitória–Trindade Ridge. The eastern temperature front of the eddy was first thought to be the inshore flank of the Brazil Current, but it turned out to be a superposition of the Brazil Current and the Vitória eddy.

In this paper, a fairly unique dataset including data from different platforms and instruments are used to describe the Vitória eddy. To our knowledge, no other reports are available that describe the anatomy of a cold eddy and its interaction with the Brazil Current in the area between the Vitória–Trindade Ridge and Cabo Frio. Furthermore, some of the eddy's physical characteristics such as its high oxygen content (see Fig. 2d) suggest that the eddy might have a significant impact on the local biology (Ring Group 1981) including the fishing industry.

a. Dataset

The dataset analyzed in this paper has three major components: (a) hydrographic data, (b) drifting buoy observations, and (c) satellite imagery.

Corresponding author address: Ms. Claudia Schmid, Institut für Meereskunde an der Universität Kiel, Düsternbrooker Weg 20, Kiel D-24105, Germany.
E-mail: cschmid@ifm.uni-kiel.d400.de

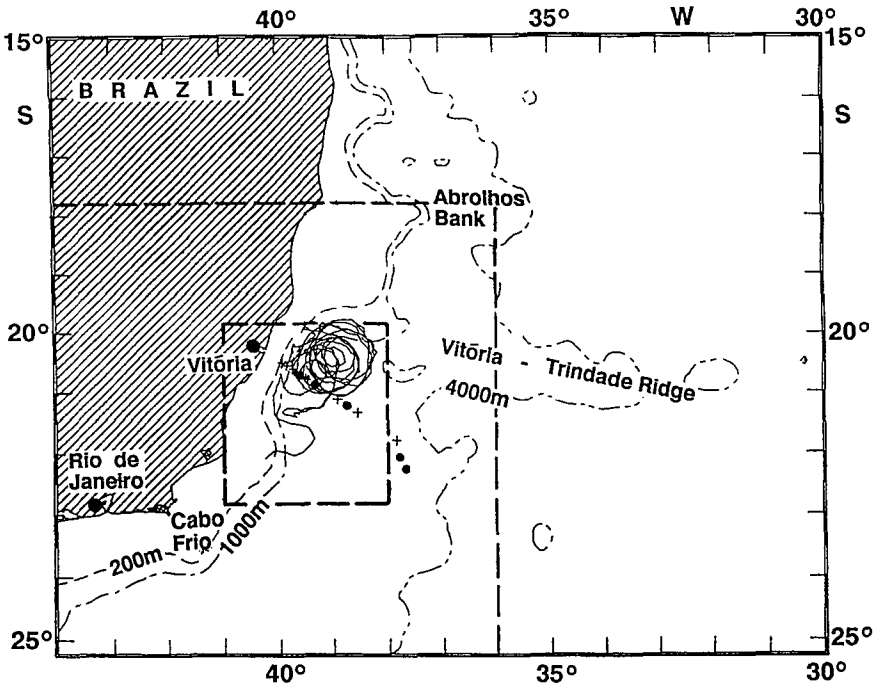

FIG. 1. Position of hydrographic stations during METEOR Cruise 15/2 and the trajectories of the drifters launched during the cruise (Brügge 1992) together with bottom topography. The large frame describes the area covered by the satellite images (Fig. 11) and by Fig. 14. The small frame marks the area used for the maps of the drifter data.

1) HYDROGRAPHIC DATA

During the second leg of the METEOR 15 Cruise, nine CTD stations were supplemented by eight XBT drops. The quality of the CTD data was routinely monitored using bottle samples during the previous and following cruise legs. Unfortunately, a desirable calibration check for the nine CTD casts analyzed here was impossible because of bad weather delays. Therefore, an extrapolation of the calibration from previous full rosette stations was used. This might have led to a slight loss in accuracy, especially in the continuous oxygen profiles where the lack of reference bottle data is most serious. Due to the high precision in the data collected until 10 days before the Vitória eddy was encountered and during the following leg of the cruise, the CTD data are considered to be accurate within ±0.005 psu, ±0.002°C, and ±0.08 ml l^{-1} for salinity, temperature, and oxygen (Speer et al. 1992).

The XBTs measured the temperature in the upper 800 m. Under the assumption of a tight temperature–salinity relation in the South Atlantic Central Water, the XBT temperature could be transformed into salinity (Flierl 1978) with an accuracy of ±0.09 psu (±0.07 kg m^{-3}).

2) DRIFTER DATA

Ten surface drifters were deployed as part of a long-term WOCE project to observe the upper circulation of the subtropical gyre of the South Atlantic (Schäfer 1993). All drifters were launched in the early morning of 7 February 1991 along a transect 40-km long in an E–W direction, located at the western edge of the eddy. To exclude the influence of the wind-driven circulation, SPAR buoys with drogues at 100-m depth were used. These instruments contain inclination sensors that transmit drogue losses, indicated by the buoys' tilted position (Brügge 1992). The buoys measured the surface temperature at approximately 1-m depth. Drifter positions were reported through the ARGOS system approximately six times per day. The raw ARGOS fixes were interpolated to 3-h intervals, using a three-point Lagrangian interpolation routine and were smoothed by a moving average over three values. Although the drifters have a battery life expectancy of 1–2 years, most of the buoys stopped collecting usable data after a much shorter period. One reason for the loss of drifter data was the high number of fishing boats operating in the study area. For instance, one of the drifters was retrieved by a fisherman right after deployment and could be tracked into the Vitória harbor. Another drifter could not be tracked via the ARGOS system. Therefore, the dataset contains eight buoys with a total of 1506 positions at 3-h intervals. The length of the drifter time series varied between 5 and 55 days. The accuracy of the ARGOS positioning system is quoted to be about 1 km (B. Brügge 1993, personal communication).

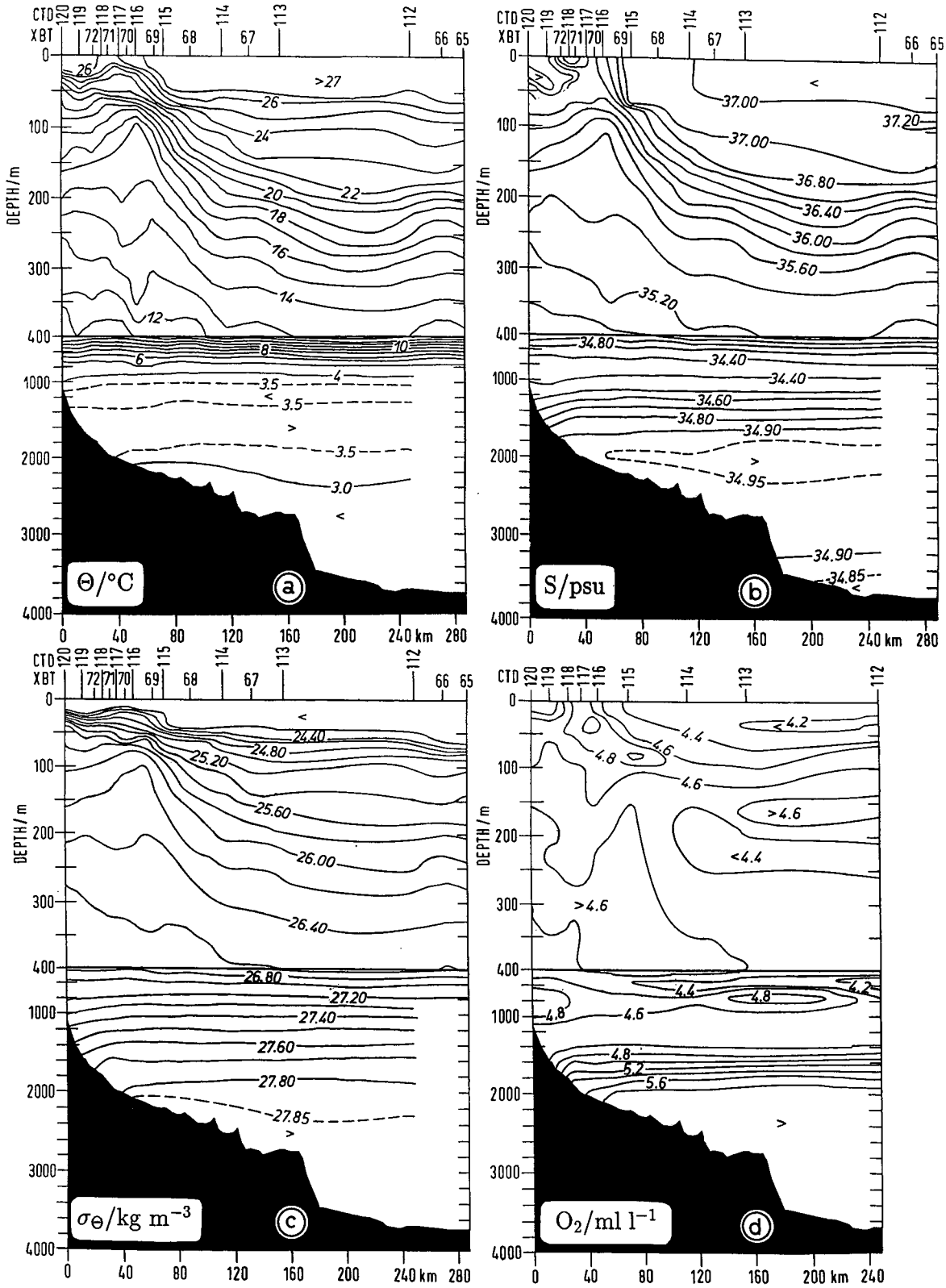

FIG. 2. Hydrographic sections across the Brazil Current: (a) potential temperature (θ), (b) salinity (S), (c) density (σ_θ), and (d) oxygen (O_2). For position of the section see Fig. 1.

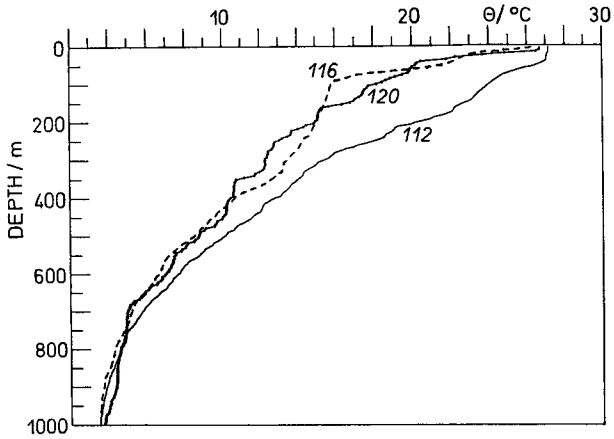

FIG. 3. Potential temperature profiles of the CTD stations east of the eddy (112), in the eddy center (116), and west of the eddy (120).

3) SATELLITE DATA

The satellite-derived sea surface temperature (SST) fields used in this study were based on data collected by the Advanced Very High Resolution Radiometer (AVHRR) flown onboard the *NOAA-11* polar orbiting satellite. SST was computed using a multichannel algorithm for AVHRR channels 4 and 5 (McClain et al. 1985). The data were then remapped to a fixed earth-based grid using a cylindrical equirectangular projection. Pixels with clouds were identified using SST thresholds (as the temperature of the top of the clouds tends to be considerably lower than that of the sea surface). To limit the amount of cloud-covered pixels, the images corresponding to 31 January 1991 and 1 February 1991 (year days 31 and 32) were composited into a single image using a "warmest pixel" approach (Podestá et al. 1991). The rest of the images were sufficiently cloud free and were not composited.

2. Analysis

a. Hydrography

Sections of potential temperature θ and salinity S (Figs. 2a,b) clearly show the structure of the Vitória eddy (stations 115–118). The eddy is characterized by cool, low-salinity water in its core. A thermal cap is apparent above the nearly homogeneous water in the Vitória eddy's core (between 100 and 300 m). This cap apparently is an indication of strong surface heating at subtropical latitudes in the austral summer. On the western side of the eddy, the thermocline is shallower (20 m) than on the eastern side (40 m), and its water is about 1°C colder. As satellite infrared images (Fig. 10) indicate, this temperature gradient might well be tied to strong coastal upwelling. The cold, relatively fresh water in the Vitória eddy might have originated mainly from an upwelling event.

A comparison of the density section (Fig. 2c) with the potential temperature and salinity sections suggests a significant temperature dependence in the upper 50 m. Below this level, potential temperature and salinity have similar influences on the density structure. The available satellite images indicate that the hydrographic section runs almost exactly through the eddy center (Fig. 11). This allows the estimation of the size of the inner core defined as the area with nearly homogeneous water. The radius of this core is about 25 km. The slope of the isopycnals (Fig. 2c) indicates that the Vitória eddy was located west of the Brazil Current at the time of observation. In the oxygen section (Fig. 2d) the near-surface maximum inside the Vitória eddy reaches far to the east while it becomes weaker. This extension to the east is interpreted as a sign of strong interaction between the Vitória eddy and the adjacent southward flowing Brazil Current.

The potential temperature difference at the eddy center (CTD station 116) is quite strong compared with the easternmost CTD station (112): The water in the Vitória eddy is up to 8°C colder (at 100 m) than the water farther east (Fig. 3). The thermal signal is apparent from the surface down to about 700 m. In contrast, the deviations between station 116 and the western potential temperature profile (CTD station 120) are smaller and they are restricted to the upper 400 m. The corresponding salinity profiles have essentially the same characteristics (not shown). In the upper 100 m the oxygen concentration in the eddy is significantly higher than in the eastern profile (Fig. 4), whereas the oxygen difference of the center profile as compared with the western profile is comparatively small. These water characteristics led to the assumption that shelf water is trapped in the Vitória eddy.

Next, geostrophic velocities are calculated. These velocities, in turn, will be used to estimate the kinetic energy of the Vitória eddy and the Brazil Current trans-

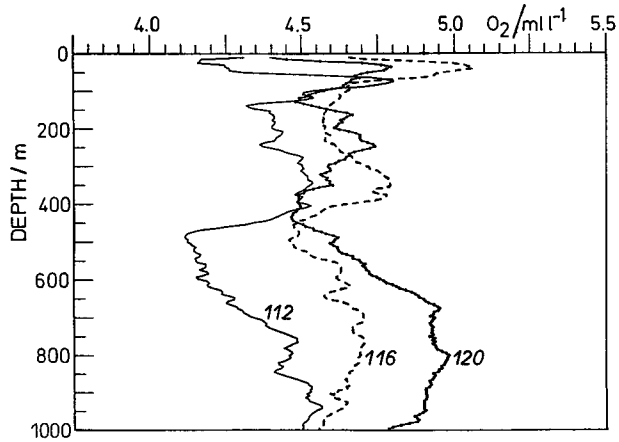

FIG. 4. Oxygen profiles of the CTD stations east of the eddy (112), in the eddy center (116), and west of the eddy (120).

port. The geostrophic transports will be compared with those estimated by other authors and the transport of water inside the Vitória eddy. First, a water mass analysis is used to find an appropriate reference level.

b. Water masses

The $\theta-S$ (Fig. 5a) and the $\theta-O_2$ (Fig. 5b) diagrams of the deepest station (number 112) show all characteristic water masses of the region. Below the upper-thermocline water (TW) lies the South Atlantic Central Water (SACW) with a nearly linear $\theta-S$ relation. This water mass is followed by the Antarctic Intermediate Water (AAIW) with a relative oxygen maximum at 750 m and a salinity minimum at 765-m depth (Peterson and Whitworth 1989; Reid 1989). The Upper Circumpolar Deep Water (UCDW) is characterized by a relative potential temperature minimum at 1115 m and an oxygen minimum at 1200 m. The North Atlantic Deep Water (NADW; maximum in θ, S, and oxygen; relative oxygen minimum) is located below the UCDW. The $\theta-S$ diagrams for the different stations (not shown) are quite similar below the thermocline, and the differences are mostly restricted to vertical shifts in the locations of the present water masses. Below 600 m the $\theta-S$ relation is almost independent of the location of the profile. In the thermocline, differences between stations are significant because atmospheric fluxes and the eastward transport of upwelled water apparently play an important role.

c. Dynamical method

Keeping in mind the water mass characteristics described above, an appropriate reference level for the geostrophic calculations can be defined. One possible reference level is 600 dbar, the boundary between the AAIW and the SACW. An alternative is the oxygen minimum at 1200 dbar, between the northward flowing AAIW and the southward flowing NADW, which is a sign for stagnation (low velocities) of the water. Both possible levels were tested. Those stations where the water depth was smaller than the depth of the reference level were not used for the geostrophic calculations, since no absolute velocities were measured on the section. The 600-dbar reference level leads to an unrealistically high geostrophic velocity of the NADW (>30 cm s^{-1}). Therefore, the 1200-dbar level was preferred, even though this makes it impossible to calculate geostrophic velocity near the shelf break.

d. Currents and transports

In Fig. 6a a section of geostrophic velocities for the remaining CTD stations (112–119) is displayed. The horizontal velocity distribution shows two speed cores of opposite signs in the upper 200 m, a clear manifestation of the cyclonic nature of the investigated Vitória eddy. The maximum in the east has a southward (negative) surface velocity of more than 50 cm s^{-1}, whereas the northward surface velocity maximum in the west is somewhat weaker (about 40 cm s^{-1}). This asymmetry can easily be explained by the superposition of the southward flowing Brazil Current and the swirl velocity on the eastern side of the Vitória eddy. From this velocity distribution and the hydrographic section, one can conclude, that the area from section km 30 to km 80 is mainly occupied by the Vitória eddy, whereas

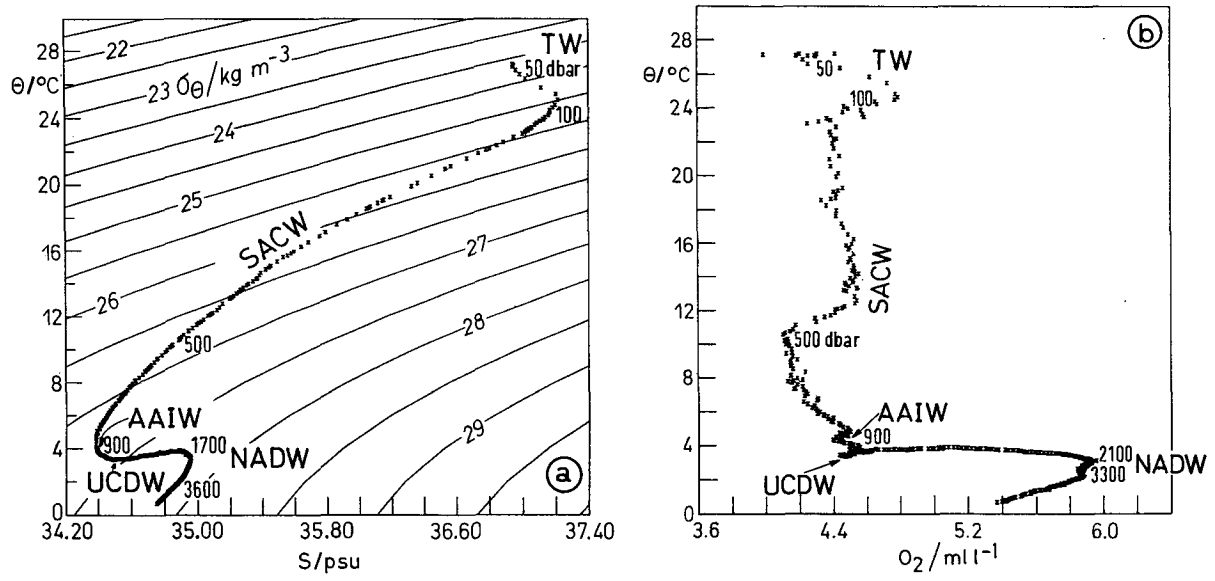

FIG. 5. $\theta-S$ diagram (a) and $\theta-O_2$ diagram (b) for the eastern flank of the Brazil Current (CTD station 112): thermocline water (TW), South Atlantic Central Water (SACW), Upper Circumpolar Deep Water (UCDW), Antarctic Intermediate Water (AAIW), and North Atlantic Deep Water (NADW).

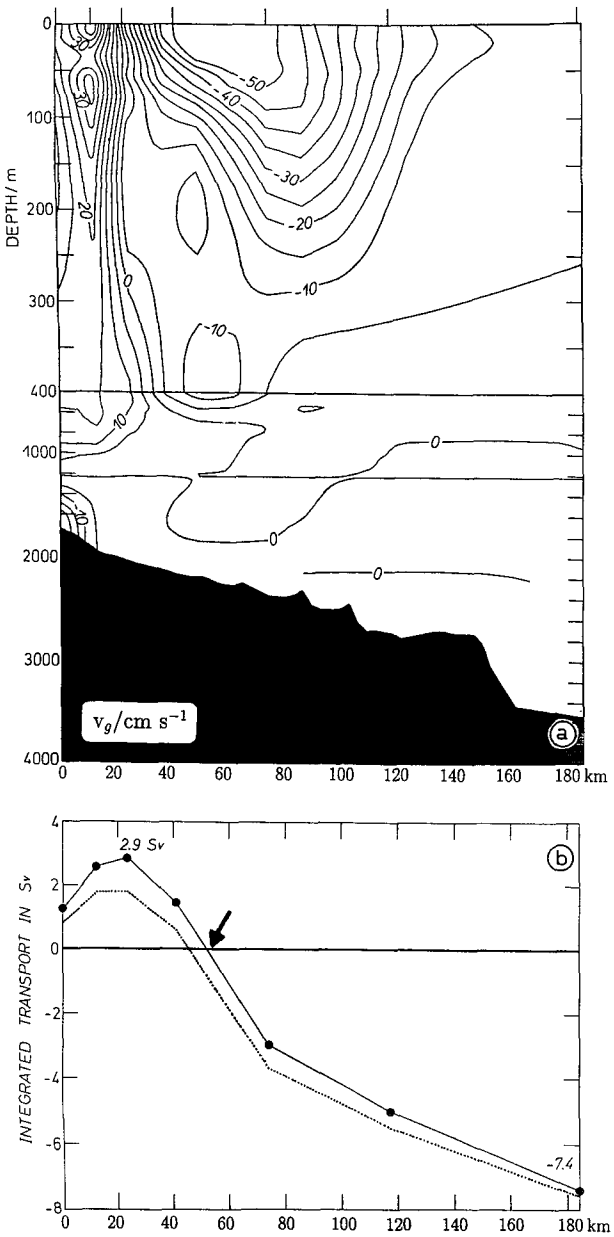

FIG. 6. (a) Geostrophic velocity (positive to the north) for stations 112–119 of the section in Fig. 1. The tick marks at the top correspond to the half points between the stations. (b) Geostrophic transport integrated from west to east in the upper 400 m (dashed line) and in the upper 600 m (solid line). The arrow marks the position where the total northward transport in the upper 600 m is compensated.

between km 80 and km 120 the Vitória eddy and the Brazil Current interact. Farther to the east the Brazil Current slowly loses strength.

The geostrophic transport in the upper 600 m for the 1200-dbar reference level has been calculated and then integrated from west to east over the whole section (Fig. 6b). The maximum cumulative northward transport of the Vitória eddy is 2.9 Sv (1 Sv $\equiv 10^6$ m^3 s^{-1}). The smallest possible radius of the eddy is defined as the distance between this maximum (which is located in the eddy center) and the position where the total northward transport is compensated (arrow in Fig. 6b). This results in an estimated radius of at least 30 km. The actual eddy radius is larger (see drifter data) because (i) the Brazil Current and the eddy overlap and (ii) the western edge of the eddy is not covered in the geostrophic section. The integrated southward transport of the whole section represents a Brazil Current transport of 7.4 Sv. This value can be compared to other published estimates of Brazil Current transport displayed in Table 1.

The Brazil Current transport derived here is the largest of the results in Table 1. However, this estimate does not seem to be extraordinarily high, since variations of the Brazil Current transport can be quite large. For example, the 6.8 Sv at 20.5°S (Evans et al. 1983) are comparable to the value of 7.4 Sv (this study). For comparison with other publications the geostrophic transport of the Brazil Current was calculated for the 600-dbar reference level as well. This value is even larger than the estimate for the 1200-dbar level. The calculated Brazil Current transport will be compared with the transport of water inside of the Vitória eddy later.

e. Kinematics and anomalies

In this section, the CTD data and the geostrophic velocity will be used to calculate energies and anomalies for the Vitória eddy. The derived quantities will then be compared with published values for similar features. The energies of the eddies are usually higher than those of the background field; therefore, they can play

TABLE 1. Brazil Current transport between 19° and 22°S. Comparison between values estimated in this study and those found in the literature.

Author	Latitude (°S)	Reference (m)	Transport (Sv)
Miranda and Castro Filho (1981)	19	~500	5.3
Evans et al. (1983)	19	500	5.3
	20.5	500	3.8
	20.5	1000	6.8
	21.7	500	4.4
Signorini et al. (1989)	20.5	500	2.9
	21.6	500	3.2
Stramma et al. (1990)	19	~600	3.7
	19.4	~560	5.7
	20	~610	1.6
	20.3	~600	1.9
Zangenberg, pers. comm. (1993)	19	600	3.2
This study	21	1200	7.4
Schmid et al. (1995)		(600)	(9.4)

TABLE 2. Kinetic energy (KE), available potential energy (APE), available heat anomaly (AHA), available salt anomaly (ASA), and the ratio KE/APE of different eddies with the radius r.

Author, description, location	AHA (10^{19} J)	ASA (10^{11} kg)	KE (10^{13} J)	APE (10^{13} J)	KE/APE	r (km)
This study, Vitória eddy	0.1	0.5	9.6	19	0.51	50
Joyce et al. (1981) cyclone, Drake Passage	1.2	2.5	34	51	0.67	50–60
Armi et al. (1989) and Schultz Tokos and Rossby (1991) meddy, NE Atlantic	2.6	18	7.9	7.5	1.10	60

an important role for the overall energy level in the ocean. Generally, the same is true for the anomalies of heat and salt. The following quantities will be calculated.

Total kinetic energy:

$$\mathrm{KE} = \frac{1}{2}\int_V \rho u_g^2 dV'$$

with

ρ density (dependent of depth z)
u_g geostrophic velocity
V volume of the eddy

Total available potential energy:

$$\mathrm{APE} = \int_V g'\rho(h - h_r)dV'$$

with

g' $(=g\Delta\rho/\rho)$ reduced gravity
$\Delta\rho$ change of ρ with depth
h_r depth of an isopycnal at the reference station (drifter 112)
h depth of an isopycnal in the eddy

Total available heat anomaly:

$$\mathrm{AHA} = \int_V \rho c_p(T - T_r)dV'$$

with

T temperature in the eddy
T_r temperature at the reference station (no. 112)
c_p specific heat

Total available salt anomaly:

$$\mathrm{ASA} = \int_V \rho(S - S_r)dV'$$

with

S salinity in the eddy
S_r salinity at the reference station (112).

The eddy is assumed to be circular with a radius of 50 km. A vertical extension down to $\sigma_\theta = 26.6$ is used for the calculations. Before integrating the values for the different stations over the eddy, they were interpolated linearly onto an equidistant grid with 1-km resolution. The anomalies of the Vitória eddy are smaller than those of the Drake Passage cyclone (Joyce et al. 1981) and the Mediterranean salt lens (Meddy Sharon: Armi et al. 1989; Schultz Tokos and Rossby 1991), Table 2. The reason for this is that the Vitória eddy is close to its origin and the water inside the eddy is not coming from regions with different water characteristics.

The APE of the Vitória eddy is smaller than that of the Drake Passage cyclone, while it is larger than that of Meddy Sharon. The same is true for the KE. The ratio KE/APE of the Vitória eddy is about one-half of the value for the Drake Passage cyclone while it is considerably smaller than that of Meddy Sharon.

f. Drifter data

While *Meteor* was heading toward Vitória all drifters were launched on 7 February 1991 (year day 38). The processing of the drifter data is described in the introduction. The trajectories of drifters 7 and 8, launched near CTD station 118, are very similar. For drifter 7, cyclonic motion for about half a revolution (inner trajectory in Fig. 7a) is followed by a 4-day long stagnation period (year days 46–50). During this period the drifter 7 drogue seems to have been moored. This is supported by echo sounding data collected during the METEOR 15 Cruise, which show bottom depths between 50 and 230 m in that area. After the stagnation, drifter 7 is caught in a big meander and drifts southward.

The next drifter pair (drifters 5 and 6) was launched adjacent to station 119, 14.4 km to the west of the previous deployment. The trajectories of both drifters are, again, very similar. The trajectory of drifter 5 encircles that of drifter 7 with a radius about twice as large (Fig. 7a). Drifter 1 was launched 47.3 km to the west of drifters 5 and 6. It moved almost directly to the east and, after a short, nearly stationary period (due to a grounded drogue), it was caught in the Vitória eddy (Fig. 7b). The radius of its second revolution (24 km) is the smallest of all observed trajectories and its swirl velocity (see Table 3) is smaller than that of drifters 7 and 8. Drifters 2, 3, and 4 were deployed between

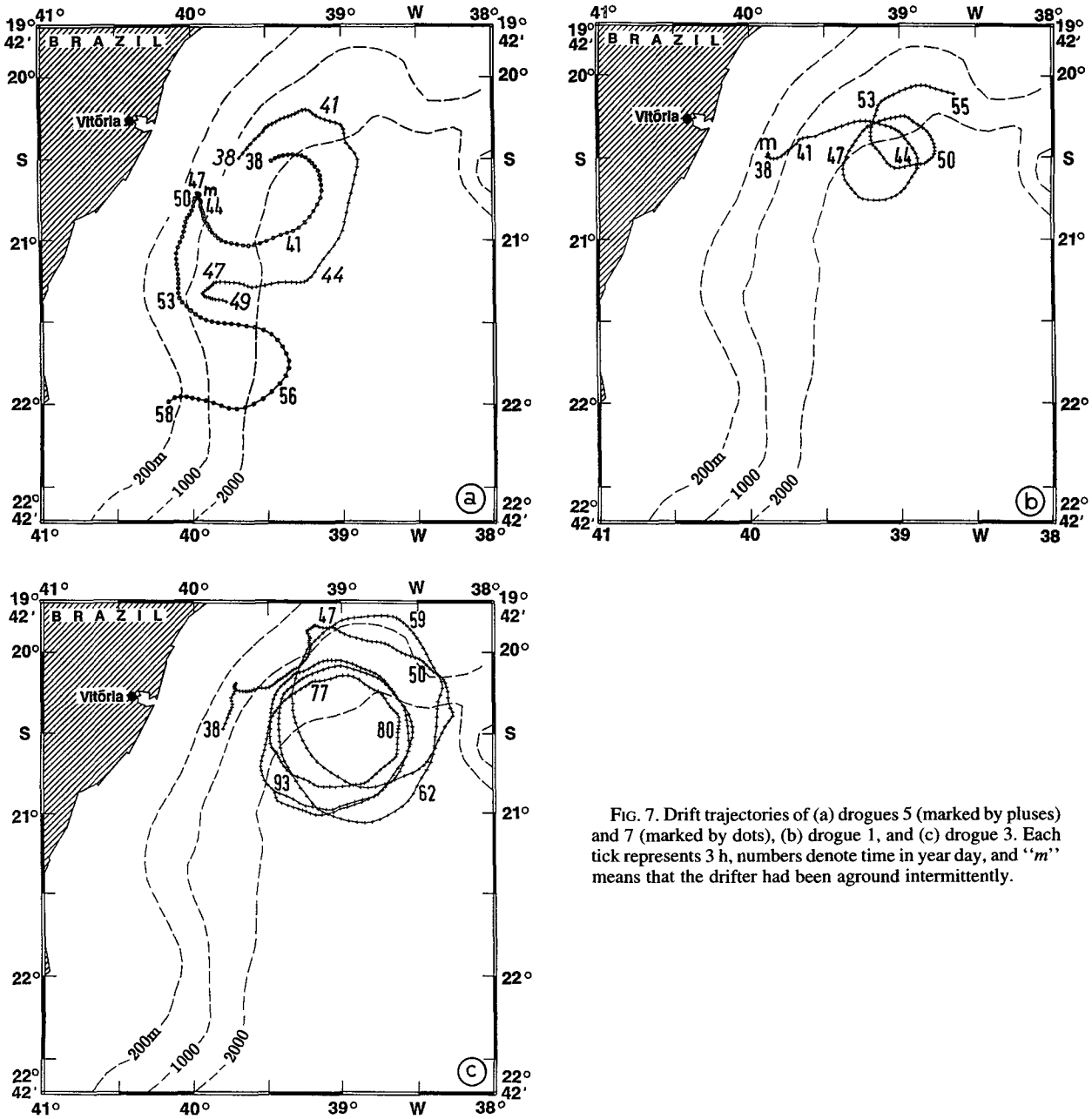

FIG. 7. Drift trajectories of (a) drogues 5 (marked by pluses) and 7 (marked by dots), (b) drogue 1, and (c) drogue 3. Each tick represents 3 h, numbers denote time in year day, and "*m*" means that the drifter had been aground intermittently.

drifter 1 and drifter 5. They entered the Vitória eddy on day 47. The trajectory of drifter 3, which stayed in the eddy for 45 days, is shown in Fig. 7c.

A plot of temperature measurements taken by drifter 3 shows a strong periodic signal with temperature changes of about 0.6°C in the first 8 days (Fig. 8a). These temperature changes agree well with the satellite image of day 38 (Fig. 11). The temperature increase (decrease) corresponds to leaving (entering) the cold water tongue in the Vitória eddy. On day 68 the temperature minimum is much weaker; this might have been caused by surface heating. After day 79 temperature changes are about 0.3°C.

Figures 8b and 8c display the smoothed Cartesian velocity components of drifter 3 while it was captured in the Vitória eddy. As expected, the velocity components show an almost sinusoidal signal since the drifter moved on a nearly circular path. The period of the drifter motion is 9.2 days. The meridional and zonal components of the drifter velocity have different amplitudes because of the eddy translation and the Brazil Current flow. A southward translation will naturally

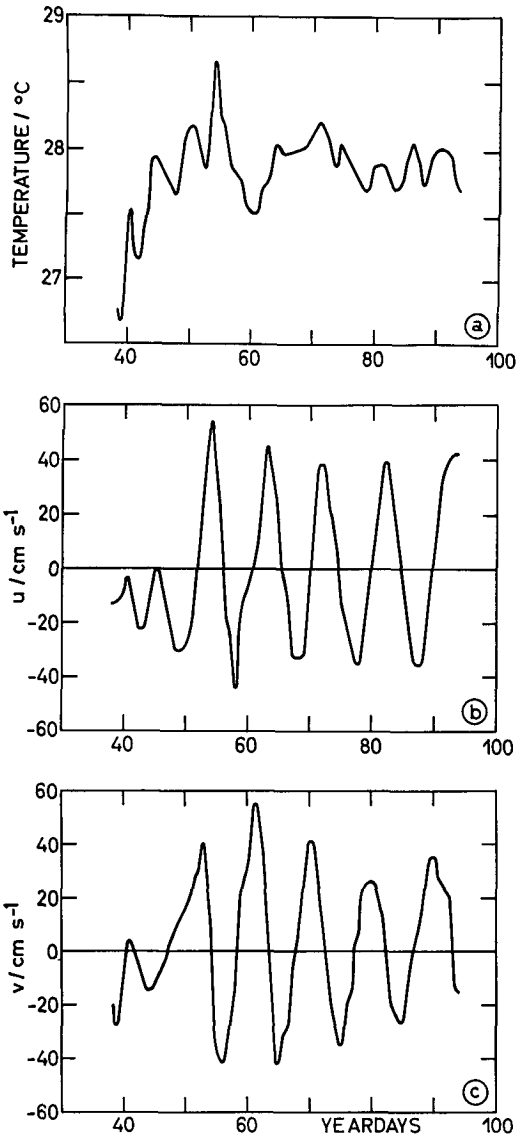

FIG. 8. Drifter number 3: (a) Temperature, (b) zonal velocity component, and (c) meridional velocity component.

lead to larger southward velocities compared with the northward and zonal velocities; the same can be observed in the case of a southward current.

A comparison of the initial velocity of drifter 8 [36.7 cm s^{-1}, 34° TC (true compass)], averaged over 4 hours beginning 5 hours after launch, with the estimated geostrophic velocity (about 20 cm s^{-1}, 37° TC) shows that the geostrophic velocities are about 40% smaller than the component of the initial drifter velocity perpendicular to the section. Geostrophically calculated velocities generally tend to underestimate the actual speed, since they do not represent small-scale currents (station spacing is of order 10 km) and exclude nonlinear processes as well as frictional effects.

g. *Eddy characteristics*

The purpose of the following calculations is to extract more information about the dynamics and the development of the Vitória eddy out of the drifter data. The trajectory of each drifter was subdivided into segments and a least squares model of the form

$$x = x_0 + u_0 t + r\cos(\omega t + \phi) \quad (1)$$

$$y = y_0 + v_0 t + r\cos(\omega t + \phi) \quad (2)$$

was fitted to each segment, where x_0, y_0 describe the position of the eddy center; u_0, v_0 are the zonal and meridional translation velocities; r is the radius of the drifter trajectory; ω the angular frequency; and ϕ the phase. The Rossby number [Ro = $U/(fr)$, where U is swirl velocity and f Coriolis parameter of the eddy center], which is a measure of the importance of the nonlinearity in the dynamical balance, can be derived once the above equations are solved.

The swirl velocities, the radii, and the Rossby numbers are displayed in Table 3. The given errors are the rms values for the estimates. For drifters 1–4, the values have been calculated for full revolutions, whereas for drifters 5–8 no full revolutions were available. This can explain the larger errors of the values for the latter trajectories. The swirl velocity increases from the eddy center to a radius of about 45 km before it decreases again (Fig. 9a).

It is commonly assumed that an eddy has solid body rotation in its core, which means that the Rossby number inside the core needs to be constant. The Rossby number of the Vitória eddy decreases with increasing radius in a nearly linear manner, possibly because the

TABLE 3. Dynamical quantities of the drifter trajectories (radius, swirl velocity and Rossby number) averaged over one full revolution (drifter 1 to 4) or one-half revolution (drifter 5 to 8).

Drifter	Yearday (1991)	Radius (km)	Swirl velocity (cm s^{-1})	Rossby number
1	45	25 ± 1	36 ± 1	0.28 ± 0.02
1	50	24 ± 2	31 ± 1	0.26 ± 0.03
2	52	52 ± 1	39 ± 1	0.15 ± 0.01
2	62	52 ± 2	45 ± 1	0.17 ± 0.01
2	74	61 ± 6	30 ± 1	0.10 ± 0.01
3	52	51 ± 1	40 ± 1	0.15 ± 0.01
3	62	52 ± 3	44 ± 1	0.17 ± 0.01
3	72	49 ± 2	38 ± 1	0.15 ± 0.01
3	82	41 ± 2	33 ± 1	0.16 ± 0.01
4	50	37 ± 2	40 ± 1	0.21 ± 0.02
4	57	48 ± 1	46 ± 1	0.19 ± 0.01
5	41	63 ± 2	37 ± 3	0.11 ± 0.02
6	42	55 ± 6	36 ± 4	0.13 ± 0.03
7	40	30 ± 2	37 ± 2	0.24 ± 0.03
8	40	35 ± 2	37 ± 5	0.20 ± 0.04

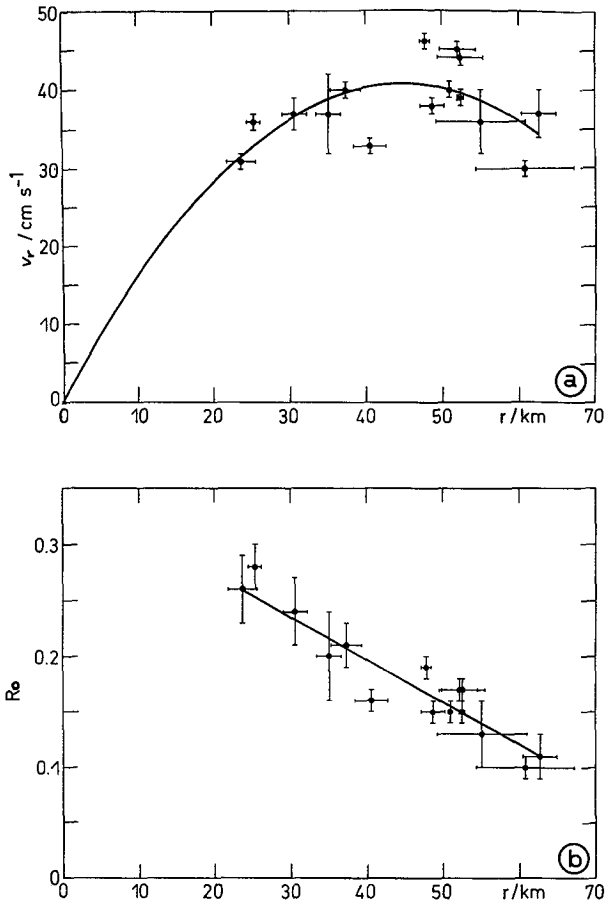

FIG. 9. (a) Swirl velocity–radius diagram and (b) Rossby number–radius diagram. The error bars are taken from Table 3, and they represent the rms values for the estimates.

drifters are outside the core (Fig. 9b). The radius of the core, therefore, cannot be larger than 25 km. Since the Rossby number for a radius of 25 km is already quite large (0.28), one can assume that the core radius is approximately 25 km, which corresponds well with the radius derived from the CTD section (see above).

In the above example the contribution of the advective terms to the flow is of order 28% of the total velocity. To a large extent this can explain the discrepancy between the measured velocities and the geostrophic velocities in the 100-m level.

The Rossby number of the Vitória eddy compares favorably with the values for Gulf Stream rings. Joyce and Kennelly (1985) reported values between 0.17 (radius 50 km) and 0.28 (radius 20 km) for the Gulf Stream warm core ring 82B.

h. Eddy translation

The translation of the Vitória eddy as derived from the drifter data is displayed in Table 4 and Fig. 13. If two drifters were in the Vitória eddy simultaneously, their center positions were averaged. The Vitória eddy translated northeastward parallel to the shelf break for the first two weeks (intervals a and b). Subsequently, it was reflected back to the south as it reached the Vitória–Trindade Ridge. On the way to the south the eddy interacted with the topography again (interval c). The volume transport of the Vitória eddy (see Table 4) has been calculated under the assumption of 50-km radius and 350-m vertical extension; it is about one-third of the Brazil Current transport.

i. Infrared satellite data

In the following, the sequence of images that were obtained prior to and simultaneously with the hydrographic observations of FS *Meteor* will be discussed. In the image of day 31/32 (Fig. 10a) a strong coastal upwelling event can be seen at 20°–21°S. It was caused by northeasterly winds (parallel to the coast; 3 to 5 Beaufort; day 30–34), which had been reported by the weather station on FS *Meteor*. Apparently, this coastal upwelling led to the formation of a meander, which developed into a cyclonic eddy that migrated toward the northeast (Figs. 10a–c).

On day 33 the thermal eddy structure was already quite strong, but the eddy was not yet separated from the upwelling region itself. Therefore, entrainment of cold water into the eddy was still possible. In the southwestern part of the eddy warm water appears to have been entrained into the eddy. The surface temperature rose quickly from less than 25°C on day 33 to almost 27°C on day 38, while the radius increased from about 42 km to approximately 45 km.

The trajectory of drifter 6 is tracking around the low temperature signal of the satellite image of day 38 (Fig. 11). This leads to the conclusion that the eddy, which can be seen on the satellite images, is identical with the Vitória eddy. The radiance sensed by satellite IR measurements originates from the upper millimeter (the "skin") of the ocean. Nevertheless, the surface signal on day 38 correlates well with the area of the lower surface temperature in the hydrographic data. The temperature signal faded out quite quickly due to seasonal surface heating and could no longer be found after day 65 (not shown).

TABLE 4. Translation of the eddy as estimated with a least squares model and transport inside the eddy (using a radius of 50 km and a vertical extent of 350 m).

Interval	Yeardays (1991)	Translation velocity (cm s^{-1})	Translation direction (deg)	Transport in eddy (10^6 m^3 s^{-1})
a	40–50	5.2	38	1.8
b	50–57	4.5	70	1.6
c	57–82	1.6	236	0.6

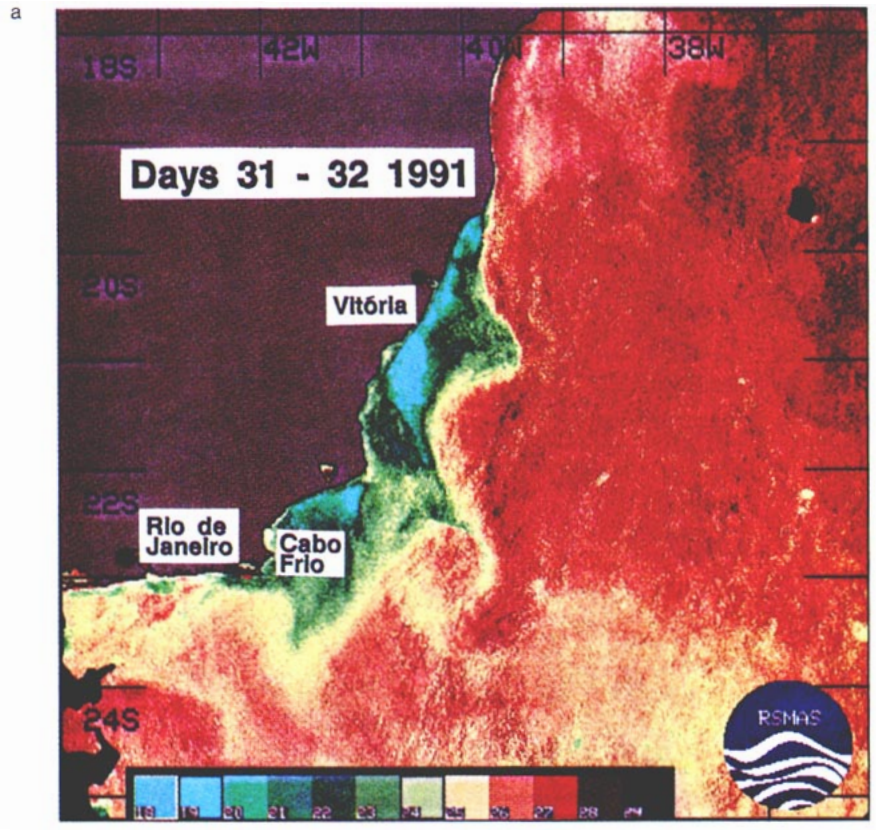

FIG. 10. Maps of the SST as computed from data collected by the Advanced Very High Resolution Radiometer in 1991 for (a) year days 31/32, (b) year day 33, and (c) year day 38.

j. Some thoughts on eddy generation and development

The described hydrography delivers some hints on the process of the generation of the Vitória eddy. A possible formation mechanism is that a strong coastal upwelling event led to a meander of the Brazil Current, which could then have developed into a cyclonic eddy. The generation of a cyclonic Gulf Stream ring begins when a large meander pinches off from the main current (e.g., Richardson 1993). A major difference between the Gulf Stream cyclones and the Vitória eddy is that the latter is on the western side of the main current, whereas the former are on the eastern side of the current.

Some insight into this fact may be gained from experimental results from Chabert d'Hieres et al. (1991). They examined the processes of eddy generation and development for a current on the Northern Hemisphere with the coast on the right-hand side in a cylindrical tank with a diameter of 13 m. The tank was filled with salty water and rotated counterclockwise. At the start of the experiment a constant flow of lighter fluid (fresh water) was released in an anticlockwise direction from a triangular opening. The current followed the tank wall and could become unstable, leading to the creation of cyclones and anticyclones (Fig. 12). In the initial phase of the development an anticyclonic eddy stayed on the coastal side of the current (Fig. 12a). This situation can remain stable during a long time (G. Chabert d'Hieres 1994, personal communication). The anticyclone could either grow (Figs. 12c,d) or disappear again (Fig. 12b). After some time the eddy detached from the meander on the left side of the current (Fig. 12e). The situation of the clockwise rotating eddy with the current on its left side (Figs. 12a,c,d) is comparable to the observed relation between the Vitória eddy and the Brazil Current (as described above).

3. Conclusions

The dataset presented here consists of CTD, XBT, drifter and satellite-derived sea surface temperatures. The data were used to describe the hydrography, dynamics, and generation of the Vitória eddy. To our knowledge, this is the first time that a cyclonic eddy has been reported directly south of the Vitória–Trindade Ridge.

b

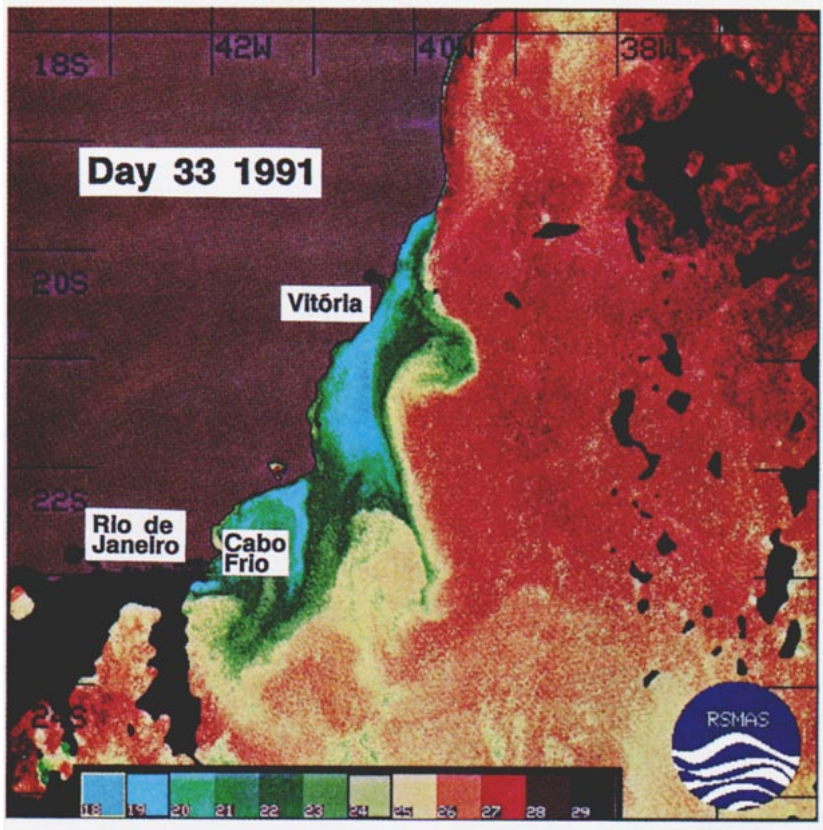

c

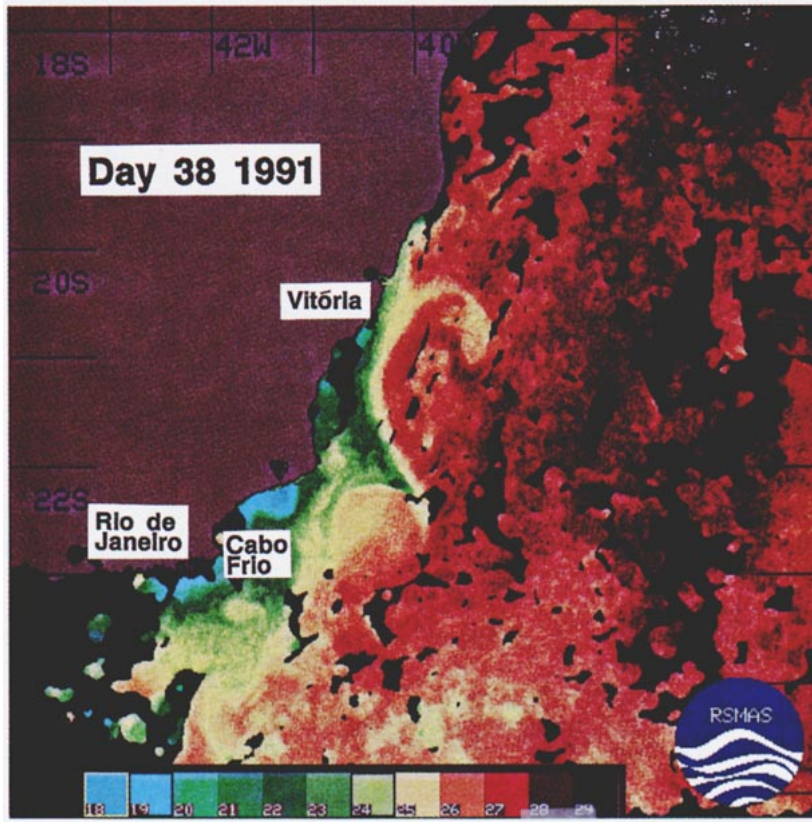

FIG. 10. (*Continued*)

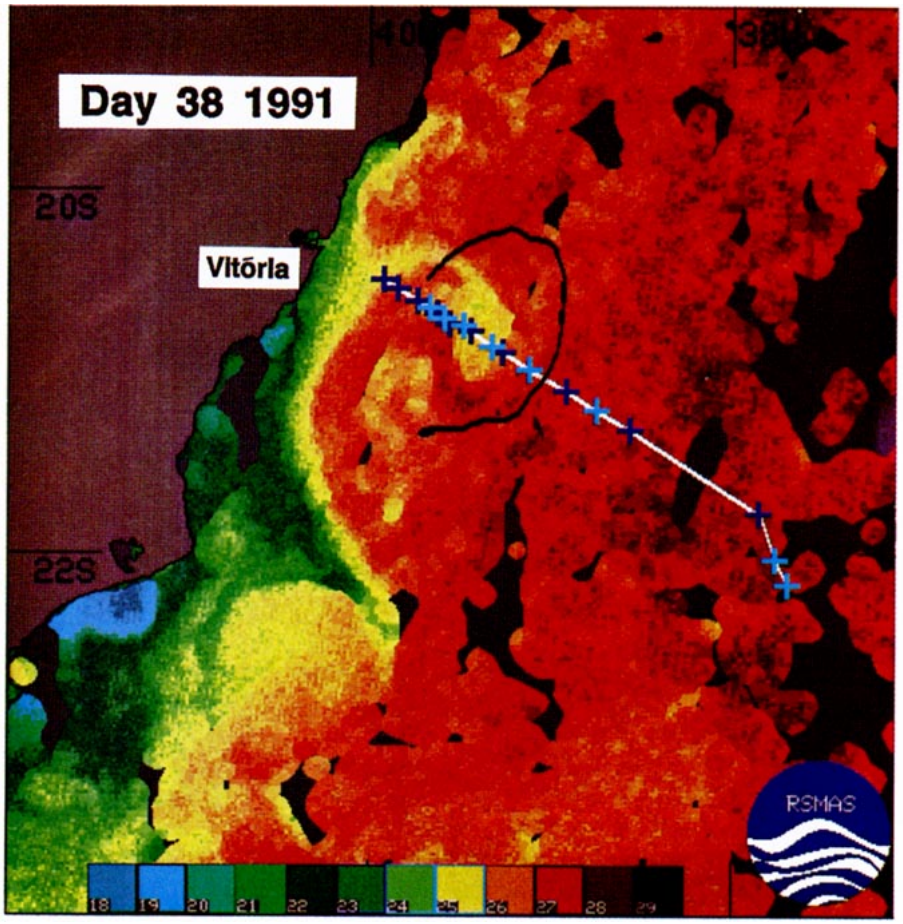

FIG. 11. Map of SST (as in Fig. 10) for year day 38 with trajectory of drifter 6 and hydrographic section (CTD: dark blue, XBT: light blue).

The kinetic and the available potential energy are comparable to those of other eddies. One example with considerably larger values for KE and APE is the Drake Passage cyclone. The available heat and salt anomalies (AHA and ASA) are smaller compared to those of other eddies since the Vitória eddy is close to its origin. The transport of water in the Vitória eddy as it migrates is about a third of the Brazil Current transport. The above results indicate that the Vitória eddy is important for the energy levels and the local circulation. However, it plays only a minor role for the heat and salt transport as long as it stays close to its origin.

The radius and the Rossby number of the Vitória eddy are quite similar to those of Gulf Stream rings; therefore they have a similar effect on the circulation dynamics.

The translation of the Vitória eddy shows some interesting characteristics. At first, the Vitória eddy translated to the northeast (intervals a and b in Table 4) before it turned back to the south (interval c in Table 4). The northeastward translation of the Vitória eddy cannot be explained by the theory of eddy translation in the open ocean (e.g., McWilliams and Flierl 1979). A cyclonic eddy in the open ocean on the Southern Hemisphere would translate in southwesterly directions in the absence of currents. Only the presence of large-scale northward currents in the upper layer would lead to northeastward translation of the upper-layer eddy (Schmid 1992). In the case of the Vitória eddy, however, only a large-scale, nearly southward current (the Brazil Current) exists. Therefore, some other dynamical process must lead to the observed northeastward

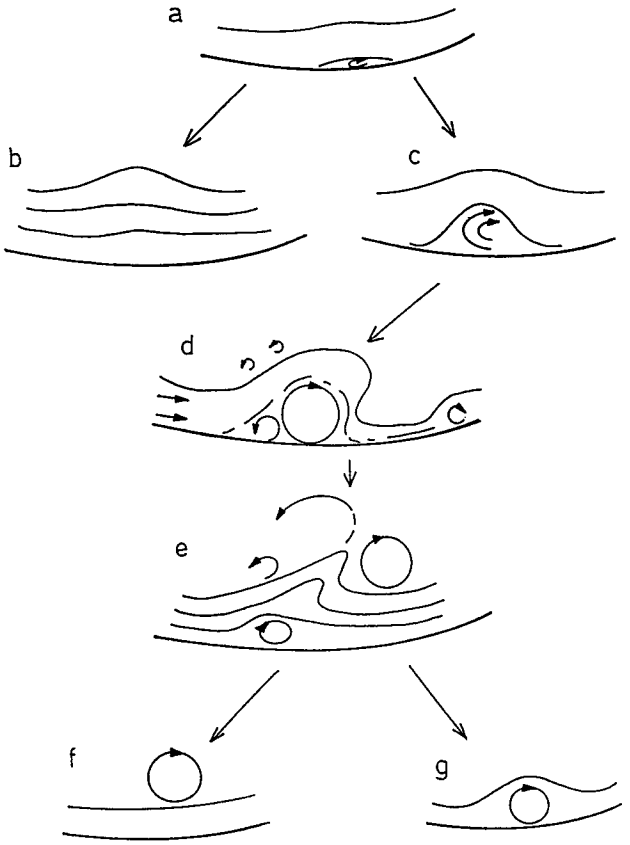

FIG. 12. Different possibilities in the evolution of an anticyclonic eddy (Northern Hemisphere). The small anticyclonic structure (a) can either disappear (b) or grow (c). In the latter case, it becomes a meander (d) composed of an anticyclonic and a small cyclonic eddy. The anticyclonic eddy may separate from the meander (e) and move independently on its own (f) or be reabsorbed by the flow (g). [Reproduced with permission from G. Chabert d'Hieres: Fig. 6 of G. Chabert d'Hieres et al. (1991).]

translation. The hypothesis is that the translation of the Vitória eddy is strongly influenced by the local topography. Nof (1983) estimated the effect of a sloping bottom on the translation of eddies. His analytical solution for the motion of an eddy on a meridional slope (S_y) is that the translation velocity is purely zonal with $c_x = g' S_y / f$. The translation for a zonal slope (S_x) can be derived similarly ($c_y = g' S_x / f$). The balancing forces consist of gravitational and Coriolis force. In the absence of other forces (e.g., currents) an eddy always moves parallel to the lines of constant depth. Therefore the Vitória eddy has to translate parallel to the bottom topography in northeasterly directions at first (intervals a and b in Table 4; see Fig. 13). The analytical translation velocities can only be estimated qualitatively because some of the assumptions are not fulfilled (i.e., vertical extent of the Vitória eddy is not small compared with the water depth). After this period the Vitória eddy suddenly translates to the southwest (interval c in Table 4; see Fig. 13). This change of direction might have been caused by the interaction of the Vitória eddy with a part of the southward Brazil Current. There

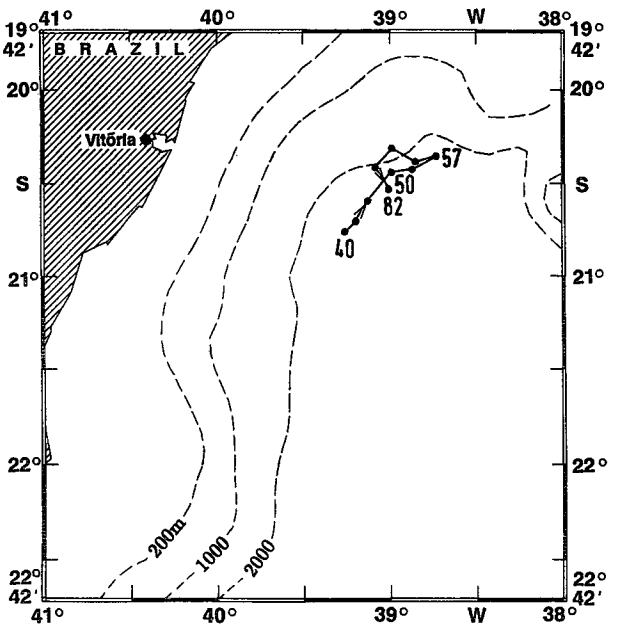

FIG. 13. Translation path of the Vitoria eddy. Dots mark the center position and the numbers denote year days.

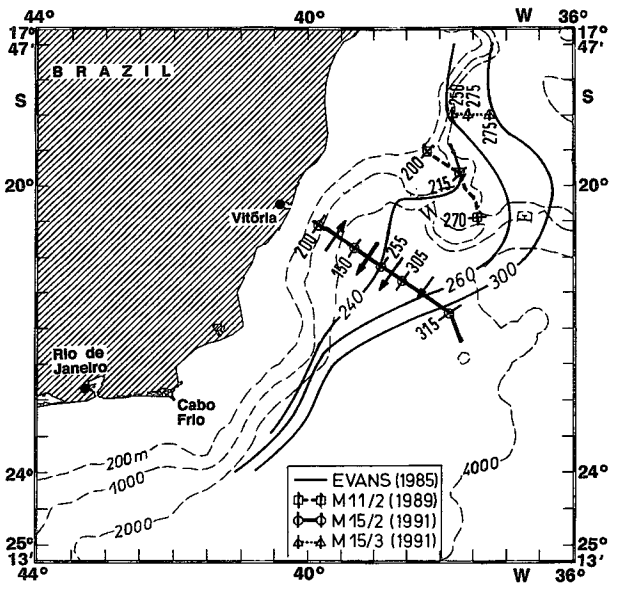

FIG. 14. Brazil Current position displayed for selected cases. Numbers denote the depth of the 15°C isotherm. Evans and Signorini (1985): From Fig. 1b. M11/2 (1989): METEOR 11/2 Cruise (from Fig. 23, Roether et al. 1990). M15/2 (1991): METEOR 15/2 Cruise, from the data analyzed here. Vectors denote the direction of the current. The long (short) vectors are for velocities greater (smaller) than 30 cm s^{-1}. M15/3 (1991): METEOR 15/3 cruise (from Fig. 22, Siedler and Zenk 1992); W: western channel and E: eastern channel.

are two processes that could be responsible for this interaction: One possibility is that the Vitória eddy penetrates into the Brazil Current as it translates to the northeast; the other possibility is that the Brazil Current moves farther to the west.

The latter is confirmed by observations of the Brazil Current near Vitória in different years are displayed in Fig. 14. One can see that the position of the Brazil Current changes considerably with time. Sometimes the greater part of the Brazil Current turns eastward north of the Vitória–Trindade Ridge, crosses the ridge at the eastern channel, and then turns back to the west where it joins the weaker western part farther south (Evans and Signorini 1985). At other times, a large part of the Brazil Current flows through the western channel of the Vitória–Trindade Ridge (METEOR 11/2). During the METEOR 15/2 Cruise the Brazil Current is farther west than reported by Evans and Signorini (1985); therefore it is more probable that it crossed the ridge in the western channel. If the Brazil Current moved farther west, an interaction with the Vitória eddy would be possible and the eddy would begin to translate to the southwest. Another possible reason for the change of direction could be a reflection of the eddy by the Vitória–Trindade Ridge.

The satellite images make it possible to give an explanation for the process of eddy generation. The observed Vitória eddy appears to have developed out of a Brazil Current meander caused by a strong coastal upwelling, therefore, cold water with low salinity was trapped in the eddy. One can conclude that the Vitória eddy had not detached itself from the Brazil Current at the time of the hydrographic observation, since the SST front was to the east of the current.

Acknowledgments. We appreciated the excellent cooperation with Captain H. Bruns and his crew aboard the *Meteor.* During the analysis phase we benefited from discussions with G. Chabert d'Hieres, D. Nof, Y. Ikeda, and W. Krauss. Figures were improved by A. Schurbohm. Support for this research was provided by grants from the Deutsche Forschungsgemeinschaft (Si 111/38-1), the Bundesministerium für Forschung und Technologie (Az. 03F0535A), and the U.S. National Science Foundation (OCE 910211). The AVHRR data were collected at Estación HRPT en Alta Resolución (Buenos Aires, Argentina) by Servicio Meteorológico Nacional, as part of a cooperative study with the University of Miami.

REFERENCES

Armi, L., D. Hebert, N. Oakey, J. Price, P. L. Richardson, T. Rossby, and B. Ruddick, 1989: Two years in the life of a Mediterranean salt lens. *J. Phys. Oceanogr.,* **19,** 354–370.

Brügge, B., 1992: Oberflächendrifter. Siedler G. and W. Zenk, 1992: WOCE Südatlantik 1991, Reise Nr. 15, 30. Dezember 1990-23. März 1991. *Meteor-Ber., Univ. Hamburg,* **92**(1), 126 pp.

Chabert d'Hieres, G., H. Didelle, and D. Obaton, 1991: A laboratory study of surface boundary currents: Application to the Algerian Current. *J. Geophys. Res.,* **96,** 12 539–12 548.

Evans, D. L., and S. S. Signorini, 1985: Vertical structure of the Brazil Current. *Nature,* **315,** 48–50.

——, ——, and L. B. de Miranda, 1983: On the transport of the Brazil Current. *J. Phys. Oceanogr.,* **13,** 1732–1738.

Flierl, G. R., 1978: Correcting expendable bathythermograph (XBT) data for salinity effects to compute dynamic heights in Gulf Stream rings. *Deep-Sea Res.,* **25,** 129–134.

Garfield, N., 1990: The Brazil Current at subtropical latitudes. Ph.D. dissertation, University of Rhode Island, 122 pp.

Joyce, T. M., and M. A. Kennelly, 1985: Upper-ocean velocity structure of Gulf Stream warm-core ring 82B. *J. Geophys. Res.,* **90,** 8839–8844.

——, S. L. Patterson, and R. C. Millard, 1981: Anatomy of a cyclonic ring in the Drake Passage. *Deep-Sea Res. A,* **28,** 1265–1287.

McClain, E. P., W. G. Pichel, and C. C. Walton, 1985: Comparative performance of AVHRR-based multichannel sea surface temperatures. *J. Geophys. Res.,* **90,** 11 587–11 601.

McWilliams, J. C., and G. R. Flierl, 1979: On the evolution of isolated nonlinear vortices. *J. Phys. Oceanogr.,* **9,** 1155–1182.

Miranda, L. B., de and B. M. Castro Filho, 1982: Geostrophic flow conditions of the Brazil Current at 19°S. *Ciencia Interamericana,* **22,** 44–48.

Nof, D., 1983: The translation of isolated cold eddies on a sloping bottom. *Deep-Sea Res.,* **30,** 171–182.

Peterson, R. G., and T. Whitworth, 1989: The subantarctic and polar fronts in relation to deep water masses through the southwestern Atlantic. *J. Geophys. Res.,* **94,** 10 817–10 838.

——, and L. Stramma, 1991: Upper-level circulation in the South Atlantic Ocean. *Progress in Oceanography,* Vol. 26, Pergamon, 1–73.

Podesta, G. P., O. B. Brown, and R. H. Evans, 1991: The annual cycle of satellite-derived sea surface temperature in the southwest Atlantic Ocean. *J. Climate,* **4,** 457–467.

Richardson, P. L., 1993: Tracking ocean eddies. *Amer. Sci.,* **81,** 261–271.

Ring Group, 1981: Gulf Stream cold-core rings: Their physics, chemistry and biology. *Science,* **212,** 1091–1100.

Roether, W., M. Sarnthein, T. J. Müller, W. Nellen, and D. Sahrhage, 1990: Südatlantik-Zirkumpolarstrom, Reise Nr. 11, 3. Oktober 1989-11. März 1990. *Meteor Ber., Univ. Hamburg,* **90**(2), 169 pp.

Schäfer, H., 1993: Statistik der Wirbelfelder im Südatlantik. Diplomarbeit, University Kiel, 70 pp.

Schmid, C., 1992: Translations- und Stabilitätsverhalten von baroklinen Wirbeln bei großskaligen Strömungen. Diplomarbeit, University Kiel, 67 pp.

Schultz, Tokos, K., and T. Rossby, 1991: Kinematics and dynamics of a Mediterranean salt lens. *J. Phys. Oceanogr.,* **21,** 879–892.

Siedler, G., and W. Zenk, 1992: WOCE Südatlantik 1991, Reise Nr. 15, 30. Dezember 1990-23. März 1991. *Meteor Ber., Univ. Hamburg,* **92**(1), 126 pp.

Signorini, S. R., L. B. de Miranda, D. L. Evans, M. R. Stevenson, and H. M. Inostroza, 1989: Corrente do Brasil: Estrutura térmica entre 19° e 25 °S e circulação geostrófica. *Bolm Inst. Oceanogr., S Paulo,* **37,** 33–49.

Speer, K., K. Schultz Tokos, and W. Erasmi, 1992: Datengewinnung und -aufbereitung während des ersten und zweiten Fahrtabschnitts. WOCE Südatlantik 1991, Reise Nr. 15, 30. Dezember 1990-23. März 1991. *Meteor Ber., Univ. Hamburg,* **92**(1), 126 pp.

Stramma, L., Y. Ikeda, and R. G. Peterson, 1990: Geostrophic transport in the Brazil Current region north of 20°S. *Deep-Sea Res.,* **37,** 1875–1886.